

**CHAPTER 5****Assessment of biodegradation kinetics and mass transfer aspects in attached growth bioreactor for effective treatment of Brilliant green dye from wastewater****5.1 Introduction**

In recent years, immobilized microorganism techniques have gained attention over free cell technique due to their advantages such as, protection of cells from washout under aerobic condition, high biomass development, and high removal efficiency (Sonwani et al., 2019; Swain et al., 2021b). The biodegradation of different organic pollutants by immobilized microorganism have been studied extensively (Patel and Gupte 2015). Various packing materials such as sodium alginate, polyurethane foam (PUF), biochar, polymeric support were used for the immobilization of microorganism (Arikan et al., 2019; Sondhi et al., 2018). In the last few years, low density polyethylene (LDPE) has been widely employed as packing media in attached growth bioreactors because it offers high surface area, good chemical resistance, and low water absorption (Swain et al., 2021b; Sonwani et al., 2021).

In the direction of attached growth bioreactor, packed bed bioreactor (PBBR) have been widely utilized for biodegradation of various organic pollutants (Bharti et al., 2019; Yadav et al., 2014). In order to scale-up these lab scale reactors to industrial scale accurately for biodegradation, the role of mass transfer correlations are important aspects for effective operation of bioreactor (Geed et al. 2018, Nath and Chand 1996). However, limited studies are available on estimation of mass

---

---

transfer correlation in attached growth bioreactors. Aksu and Bülbül 1998 , have reported correlation of mass transfer for biodegradation of phenol in packed bed reactor. Banerjee and Ghoshal (2016) have also proposed a mass transfer correlation for biodegradation of phenol in packed bed reactor using calcium-alginate beads immobilized with *Bacillus cereus AKG1 MTCC9817* as packing material.

Biofilms, which are comprised of extracellular polymeric substance (EPS) and microbial populations, are believed to play a key role in the packed bed bioreactor. EPS has a complex chemical composition that includes polysaccharides, proteins, nucleic acids, and lipids as major constituents (Mahto and Das, 2022; Naresh Yadav et al., 2021). EPS gives biofilms structural stability and keeps them metabolically active. The primary function of EPS is to facilitate microbial cell attachment to biotic and abiotic surfaces (Vandana and Das, 2021). To the best of our knowledge, there are limited studies that investigated the role of biofilm on dye biodegradation.

In this work an effort was made to investigate the role of biofilm and EPS in dye degradation. The performance of bioreactor packed with *Bacillus licheniformis* immobilized LDPE was assessed for degradation of BG dye. The effect of external mass transfer on biodegradation of dye was also evaluated. A correlation between external mass transfer coefficient and mass velocity at different flow rates was developed. The comprehensive degradation was confirmed by GC/MS analysis and a possible pathway for degradation of BG dye was deduced. Toxicity was assessed by *vigna radiata* seed for phytotoxicity and by *P. luminescence* for bacterial toxicity.

---

---

## **5.2 Materials and method**

### **5.2.1 Bacterial growth evaluation and EPS extraction**

The bacterial was cultured in nutrient broth (NB) diluted with various concentrations of BG dye (0, 20, 40, 60, 80, 100, and 200 mg/L) at pH 8.0 and 35°C to obtain the bacterial growth curve. The growth curve was constructed by taking readings of the OD at 600 nm at every 12 hours of interval. The duration needed for bacteria to grow to their highest potential was used for subsequent experiments. Typically, the transition of microorganisms from a planktonic to a sessile state results in the formation of biofilms (Biofilm formation). Microorganisms and their associated extracellular polymeric substances (EPS) are referred to structurally as biofilm systems (Extracellular polymeric). Protein, polysaccharides, and DNA make up the majority of these EPS, which provide resistance to outside stress. For EPS evaluation, biofilm sample was collected after the immobilization operation and allowed to mature in nutrient broth for various concentrations of BG dye. After 48 hr of incubation, 30 mL of the sample was taken out and centrifuged at 4000 rpm for 10 min at 4°C. After discarding the supernatant, the cell pellet ended up suspended in saline water (0.5 %) and kept at 60°C for 30 min. Then the sample was centrifuged at 12000 rpm for 15 min at 4°C and the supernatant was taken for EPS evaluation. The protein content was measured via spectrophotometer (Model: ELICO SL 159) using a modified Lowry method (LOWRY et al., 1951) and polysaccharides were evaluated using phenol – sulfuric method (Dubois et al., 1951).

### **5.2.2 Experimental setup, immobilization, and operation of PBBR**

The bioreactor setup (PBBR) used in this study was made of a borosilicate glass reactor, peristaltic pump (Milton Roy A-11 SS), air pump (XP-AC-24L), feed tank, rotameter, silicon

---

---

tubing and two sampling port (**Fig. 5.1**). The height and internal diameter of the PBBR was 100 cm and 5 cm, respectively with total volume of 1.9 L (working volume ~ 1.0 L) as mentioned in **Table 5.1**. Air was supplied through stone diffuser to maintain aerobic condition in the reactor. The air was filtered by 0.22  $\mu\text{m}$  filter and flow rate of air was controlled by a rotameter. LDPE cubes of density 0.91  $\text{g}/\text{cm}^3$  was used as a packing material in the PBBR. LDPE sheet was cut into cubes (1 cm  $\times$  1 cm  $\times$  1 cm), washed with 70% ethanol and finally dried at 50  $^{\circ}\text{C}$  in an oven (Swain et al., 2021b). The dried cubes of LDPE are then packed into the reactor. For the immobilization, acclimatized microbial consortium was inoculated on LDPE carrier and the reactor was operated in batch mode with MSM and microbial consortium for 20 days to ensure the formation of biofilm on LDPE surface. The confirmation of biofilm developed on the surface of LDPE was done both visually and using a Scanning Electron Microscope (SEM). The final experiment was carried out at 200 ppm of BG dye in wastewater. The pH and temperature was maintained at  $8.0 \pm 0.5$  and  $35 \pm 1^{\circ}\text{C}$ , respectively. Flow rates were varied from 5 to 20 mL/min and outlet samples were drawn from the top of the reactor at regular interval to evaluate the degradation of BG dye.

### 5.2.3 Development of model for mass transfer study

In PBBR, immobilized with micro-organism on porous carrier, generally two transport phenomenon occurs. First phenomenon is transportation of substrate due to difference in concentration of bulk phase and outer surface of immobilized porous support and the second is substrate internal diffusion and reaction in the biofilm (Kathiravan et al., 2010; R. K. Sonwani et al., 2019). As stated by the two film theory, a hypothetical laminar film formed adjacent to the boundary of the surface in proximity of flowing fluid (Geed et al., 2018a). The substrate required to be transported to that region, which mainly occurs due to molecular diffusion.

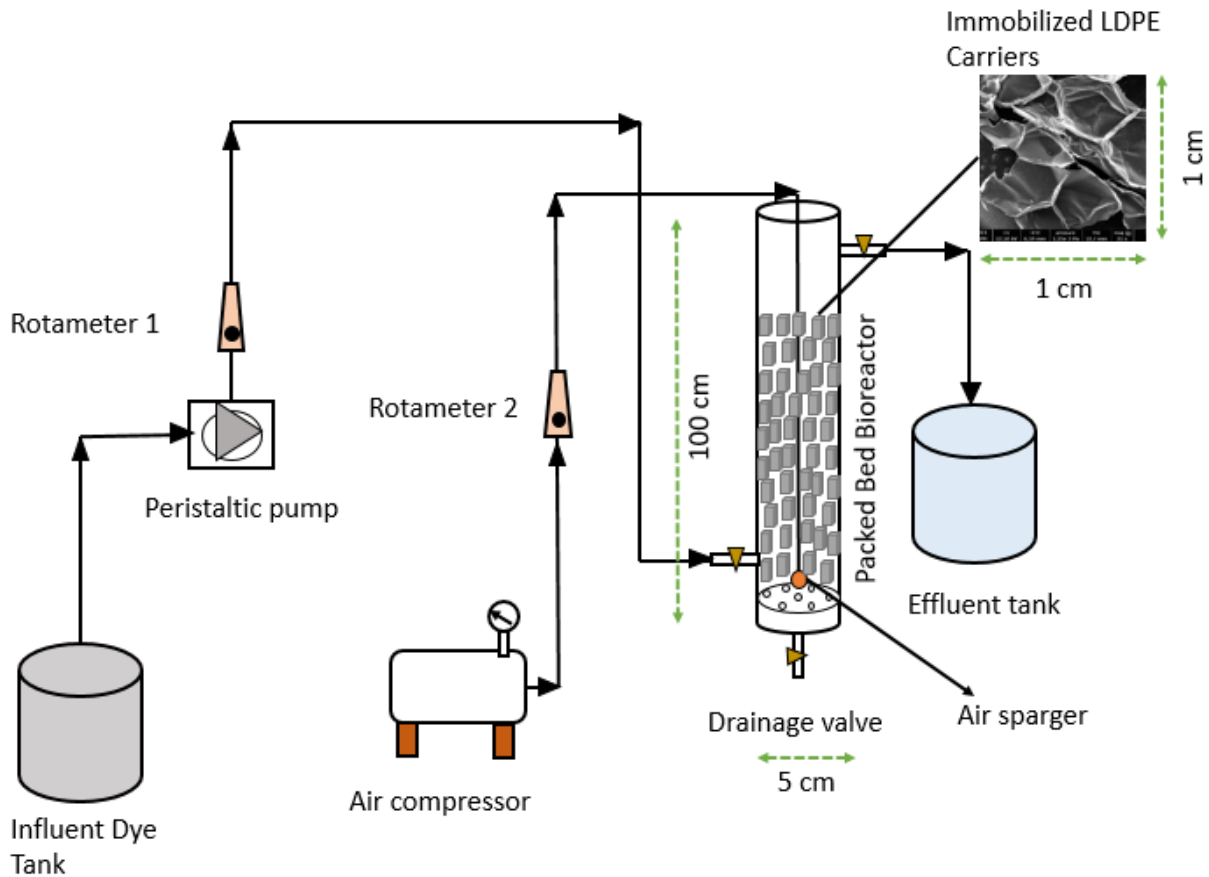


**Fig. 5.1** Schematic diagram of reactor setup for removal of BG dye

**Table 5.1** Dimensional specification and condition of PBBR for degradation of BG dye

Parameters	Units	Values
Reactor material	-	Borosilicate glass
Diameter of reactor	cm	5.0
Height of reactor	cm	100
Total volume	mL	1900
Packing material	-	LDPE
Equivalent diameter of packing material	cm	1.0
Porosity	-	0.31
pH of solution	-	$8.0 \pm 0.5$
Temperature	$^{\circ}\text{C}$	$35 \pm 1$
Inlet concentration of dye	mg/L	200

---



---

Mass of immobilized biomass	g	11.5
Inlet flowrate	L/h	0.3 – 1.2

---

### 5.2.3.1 BG biodegradation rate constant

Assuming steady state without axial dispersion, plug flow behavior and cubical shape of packing material, the material balance for brilliant green degradation in PBBR can be given by the following equation (R. K. Sonwani et al., 2019; Tepe and Dursun, 2008).

$$\left(\frac{hQ}{W}\right) \frac{dB}{dZ} = -r \quad (5.1)$$

where,  $Q$ ,  $W$ ,  $h$ , and  $r$  are the volumetric flow rate of BG dye (L/h), weight of dried immobilized cells (g), height of the packed bed reactor (cm), and biodegradation (BG dye) rate (mg/g.h), respectively.  $dB/dZ$  is the concentration gradient with respect to the reactor length (mg/L.cm). Assuming biodegradation rate is of first-order, the rate ( $r$ ) can be represented in terms of first-order rate constant ( $k_p$ ) and BG dye concentration in the column as given by Eq. (5.2) (Aksu and Bülbül, 1998):

$$r = k_p B \quad (5.2)$$

Integrating the Eq. (5.1) after substituting  $r$  defined boundary conditions (at  $Z = 0$ ;  $B = B_{in}$  and at  $Z = h$ ;  $B = B_{out}$ ) the following equation can be obtained

$$k_p = \left(\frac{Q}{W}\right) \times \ln\left(\frac{B_{in}}{B_{out}}\right) \quad (5.3)$$

Where  $B_{in}$  and  $B_{out}$  are the initial and final BG dye concentration (mg/L), respectively.

### 5.2.3.2 Assessment of mass transfer and film diffusion coefficient

As fluid flow through immobilized bed of support particles, the flow is considerably low in region developed adjacent to the outer surface of the support media (Nath and Chand, 1996; Sheeja and Murugesan, 2002) which results formation of a stagnant fluid film in the region near the periphery of packing material. The biodegradation reactions mainly occur in this film and at the surface of support media. The substrate (i.e. BG dye) transported through that film by molecular diffusion and rate of substrate transportation plays important role in biodegradation rate. For very slow substrate transportation, the external mass transfer resistance may be very high and limiting rate step (Banerjee and Ghoshal, 2016).

The substrate diffusion rate in the biofilm can be represented by Eq. (5.4)

$$r_m = k_m a_m (B - B_s) \quad (5.4)$$

where,  $r_m$  represents BG dye diffusion rate (mg/g.h),  $k_m$  represents mass transfer coefficient (L/cm<sup>2</sup>.h) and  $a_m$  represents the surface area per unit weight of dried immobilized cells (cm<sup>2</sup>/g).  $B$  is the BG dye concentration in liquid bulk and  $B_s$  is BG dye concentration on the surface of immobilized LDPE (mg/L).

The value of  $a_m$  can be calculated by Eq. (5.5):

$$a_m = \frac{6(1-\varepsilon)}{\rho_p d_p} \quad (5.5)$$

where  $d_p$  is equivalent diameter of packing material (cm),  $\rho_p$  is density of packing material (g/cm<sup>3</sup>) and  $\varepsilon$  is bed voidage.

The Eq. (5.6) represents biodegradation rate (r)

$$r = k_s a_m B_s \quad (5.6)$$

where  $k_s$  is the biodegradation rate constant (L/cm<sup>2</sup>.h). At steady state, all dye diffused from bulk phase to biofilm consumed in the biofilm and at the surface of packing media. Under this condition the rate of diffusion will be equal to rate of biodegradation of dye Eq. (5.4) and Eq. (5.6).

The observed biodegradation rate ( $k_p$ ) can be written as after rearrangement:

$$\frac{1}{k_p} = \frac{1}{k_m a_m} + \frac{1}{k_s a_m} \quad (5.7)$$

From above equation,  $k_m$  can be written as:

$$k_m = \frac{k_p k_s}{(k_s a_m - k_p)} \quad (5.8)$$

### 5.2.3.3 Model development for brilliant green dye degradation

The coefficient of mass transfer ( $k_m$ ) is generally depends upon the parameters like liquid flow rate, reactor diameter ( $D$ ) and fluid properties (i.e. feed density, substrate diffusivity and feed viscosity), which can be expressed by a dimensionless group (Dizge and Tansel, 2010;):

$$J_D = \frac{k_m \rho}{G} \left( \frac{\mu}{\rho D_f} \right)^{\frac{2}{3}} = K N_{Re}^{-(1-n)} \quad (5.9)$$

where  $J_D$  is the colburn factor which is a function of  $N_{Re}$  (Reynolds number).  $\rho$ ,  $\mu$ ,  $G$ , and  $D_f$  are density of inlet wastewater (g/cm<sup>3</sup>), viscosity (g/cm.s), mass velocity (g/cm<sup>2</sup>.h), and brilliant green diffusivity (cm<sup>2</sup>/s), respectively.

The mass velocity of fluid ( $G$ ) can be obtained by following equation:

$$G = \frac{60Q\rho}{A\varepsilon} \quad (5.10)$$

where  $Q$  is the volumetric flow rate of BG dye (mL/min) and  $A$  is the cross sectional area of the PBBR (cm<sup>2</sup>).

From Eq. (5.9),  $k_m$  can be simplified as

$$k_m = NG^n \quad (5.11)$$

Where,

$$N = \left(\frac{K}{\rho}\right) \left(\frac{\mu}{\rho D_f}\right)^{\left(\frac{-2}{3}\right)} \left(\frac{d_p}{\mu}\right)^{n-1} \quad (5.12)$$

Substituting Eq. (11) into Eq. (7)

$$\frac{1}{k_p} = \left(\frac{1}{Na_m}\right) \left(\frac{1}{G^n}\right) + \frac{1}{k_s a_m} \quad (5.13)$$

To calculate the external surface area for mass transfer ( $a_m$ ), the Eq. (5.13) plotted between  $1/k_p$  vs.  $1/G^n$  for various value of  $n$ . The values of intercept ( $1/k_s a_m$ ) and slope ( $1/Na_m$ ) can be obtained from straight line plot and used to calculate  $a_m$  for different value of  $K$  and  $n$ . The calculated value of  $a_m$  was compared with the experimentally obtained value of  $a_m$  to suggest the most accurate set of  $n$  and  $K$  for mass transfer correlation of BG dye biodegradation in PBBR.

#### 5.2.4 Biodegradation kinetics

The relationship between microorganisms specific growth rate ( $\mu$ ) and substrate concentration ( $S$ ) is a useful tool in biotechnology. The fundamental presumption of biodegradation kinetics is that substrates are degraded through catalyzed reactions carried out by the active biomass (Okpokwasili and Nweke, 2006).

An empirical model first proposed by Monod (Eq. 5.14) has dominated the concept of microbial growth kinetics. The Monod model popularized the idea of a growth limiting substrate.

$$\mu = \frac{1}{X} \frac{dx}{dt} = \frac{\mu_{max}S}{K_s+S} \quad (5.14)$$

where  $\mu$  is specific growth (per day),  $K_s$  denotes as half-saturation constant (mg/L),  $S$ ,  $X$ , and  $t$  are initial substrate, microbial cell concentration (mg/L), and time (day), respectively. However, at higher substrate concentrations, this equation fails to explain the inhibitory growth of microorganisms. Hence, in such cases Andrew-Haldane and Han–Levenspiel model could be used to describe the growth kinetics.

Andrew – Haldane model (Eq.) includes an inhibitory constant ( $K_i$ )

$$\mu = \frac{\mu_{max}S}{K_s+S+\frac{S^2}{K_i}} \quad (5.15)$$

The parameters  $\mu_{max}$  and  $K_s$  in Monod's model relate the growth rate to the concentration of a single growth-limiting substrate. Additionally, Monod connected the yield coefficient ( $Y_{X/S}$ ) with the specific rates of biomass growth ( $\mu$ ) and substrate utilization ( $q$ ) (Das et al., 2021).

$$q = \frac{1}{X} \frac{dx}{dt} = \frac{q_{max}S}{K_s+S} \quad (5.16)$$

$$\frac{dS}{dt} = - \frac{q_{max}SX}{K_s+S} \quad (5.17)$$

$$\frac{dX}{dt} = - Y_{X/S} \frac{dS}{dt} \quad (5.18)$$

$$\mu = Y_{X/S} q \quad (5.19)$$

---

---

In order to explain substrate stimulation at low concentrations and substrate inhibition at high concentrations, Han and Levenspiel (1988) first proposed a generalized Monod type model.

$$\mu = \frac{\mu_{max}S\left[1-\left(\frac{S}{S_m}\right)\right]^n}{S+K_s\left[1-\left(\frac{S}{S_m}\right)\right]^m} \quad (5.20)$$

where,  $S$  is denoted for substrate concentration (mg/L),  $S_m$  is denoted for critical inhibitor concentration (mg/L),  $n$  and  $m$  are experimental constants. The experimental data were fitted in Han and Levenspiel's model using the trial and error method in order to assess the various kinetic parameters of the biodegradation study.

### 5.3 Results and discussion

#### 5.3.1 Effect of BG dye on growth characteristics and composition of EPS

The bacterial growth was estimated for various concentration of BG dye by plotting optical density (OD<sub>600</sub>) vs process time (**Fig. 5.2(a)**). The results showed that bacteria grown in a dye-free medium was more effectively than those grown in dye-amended medium. Furthermore, the bacterial growth curve demonstrated the variation with various BG dye concentrations. The maximum bacterial growth was obtained after 48 hrs of incubation time at different concentration of BG dye (Control, 50, 100, 150, 200 mg/L). In addition, Roy et al. (2020), observed that two *Enterobacter* species showed their maximum growth at 48 hrs for the degradation of the Malachite Green (MG) dye. Therefore, further experiments have been conducted using the 48 hrs treatment period.

The evaluation of EPS was carried out post-immobilization in terms of the level of protein (PN) and polysaccharides (PS) after its exposure to BG dye solutions (**Fig. 5.2(b)**). The level of PN

were increased with increasing the BG dye concentrations from 50 - 200 mg/L, while PS only increased at 50 and 200 mg/L. The amount of PS and PN at 50 mg/L of BG dye concentration was  $20 \pm 1.5$  mg/g VSS and  $100 \pm 5$  mg/g VSS, respectively. The PS content was decreased to  $15 \pm 1.5$  mg/g VSS and PN content also decreased to  $95 \pm 5$  mg/g VSS at 100 mg/L of BG dye concentration (EPS 110 mg/g VSS). A similar phenomenon is also observed by Barathi et al. (2022). The highest EPS production of  $\sim 150$  mg/g VSS was obtained at 200 mg/L of BG dye solution. EPS is an essential component in the matrix of microbial aggregation, which gives bacteria a stable environment and shields them from toxic substances and hydraulic shear force (Gao et al., 2021). Polysaccharides are essential for protecting the biofilm against the toxic environment. It was clearly visible that as the dye concentration was increased, PS level also increased to ensure the structural stability of biofilm (**Fig 5.2(b)**). The findings indicated that high levels of BG dye disrupted the EPS and inhibited the development of biofilms, which had an impact on the dye decolonization procedure.

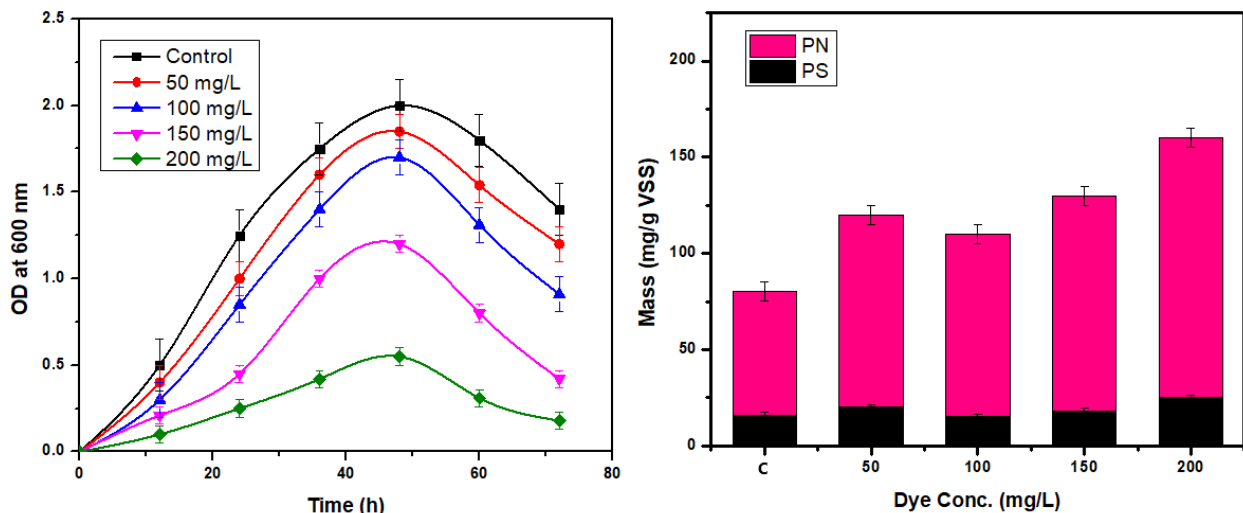


**Fig. 5.2** (a) Bacterial growth curve at various BG dye concentrations (50, 100, 150, 200 mg/L) (b) Effect of BG dye concentration on protein and polysaccharide levels.

---

---

### 5.3.2 Effect of flow rate on BG dye degradation

In PBBR, biodegradation studies were carried out at flow rates of 0.3, 0.6, 0.9, and 1.2 L/h while maintaining an initial concentration of BG dye 100 mg/L. **Table 5.2** represents the experimental value of biodegradation rate constant  $k_p$  at different flow rates (obtained from Eq. 5.3). At the flow rate of 0.3 L/h, the  $k_p$  was found to be 0.04984 L/g h. The low value of  $k_p$  could be due to mass transfer resistance in the liquid film (Tepe and Dursun, 2008). However, as the flow rate was increased from 0.3–1.2 L/h, the value of  $k_p$  increased from 0.04984 – 0.07967 L/g.h (**Fig 5.3**). This could be due to increase in turbulence at high flow rate which facilitate the better mass transfer and reduce the mas transfer resistance (Banerjee and Ghoshal, 2016). **Table.5.2** and **Fig. 5.3** clearly show that the biodegradation rate constant  $k_p$  increased with increasing flow rate. Similar observations were recorded by other researchers (Banerjee and Ghoshal, 2016; Mudliar et al., 2008; Sonwani et al., 2019). Although the value of  $k_p$  was increased at higher flow rates, the %degradation of dye was decreased. The maximum degradation of BG dye (85.2%) was obtained at 0.3 L/h and it was further decreased (53.4%) at 1.2 L/h. However, elimination capacity (EC) was increased from 25.56 mg/L.h (at 0.3 L/h) to 55.92 mg/L.h (at 1.2 L/h). This phenomenon can be observed due to reactor control mechanism. Maximum degradation occurs at lower flow rate because of longer retention time for dye molecules to interact with immobilized bacteria (Chen et al., 2005). As the flow rates increases the corresponding retention time decreases, which leads to low degradation of dye molecules. EC increased with the increasing flow rates, this can also be explained through bioreactor control mechanism. The majority of the surface that an enzyme is attached to when it is immobilized on a porous support is typically found inside the particle. As a result, the enzyme attached to the interior surface will likely have the largest impact on the rate of

catalyzed reaction. To reach the enzyme for conversion to product, the substrate must not only diffuse through the external film surrounding the particle, but also through the pores of the solid. At low flow rate, diffusion through biofilm will be less, resulting in mass transfer control mechanism as the pore diffusion restrict the overall conversion. As the flowrate increases, the diffusion of dye molecule through the biofilm surface increases, thus control mechanism shifted from mass transfer to bio-reaction control mechanism resulting in high EC.

Similar degradation phenomenon is also observed by several researchers. Swain et al., 2021a observed 87.31% color removal at optimized process conditions in PBBR. Sonwani et al., 2020a observed 95.7% of removal efficiency for Congo red dye removal in moving bed bioreactor. In another study, Tripathi et al., 2023b observed 91.2% of removal efficiency for brilliant green dye biodegraded in PBBR. Bharti et al., 2019 has reported 96.2% of methylene blue dye at optimize process condition (inoculum size of 3 mL, temperature of 30°C, 150 ppm, and time of 5 days).

### 5.3.3 Study of external mass transfer effect

The effect of external mass transfer on BG dye biodegradation was investigated at various flowrates (0.3 – 1.2 L/h) by analyzing values of Reynolds number ( $N_{Re}$ ) and mass velocity ( $G$ ). The experimentally obtained data of  $d_p = 1$  cm,  $\mu = 0.0082$  g/cm.s,  $\varepsilon = 0.31$ ,  $D_f = 3.11 \times 10^{-6}$  cm<sup>2</sup>/s,  $\rho = 1.12$  g/cm<sup>3</sup> and  $A = 19.625$  cm<sup>2</sup> were used to calculate mass velocity and dimensionless number ( $N$ ). **Table 5.2** represents the value of  $k_p$ ,  $1/k_p$ ,  $G$  and  $1/G^n$  at various values of  $n$  ( $0 < n < 1$ ). The slopes and intercepts corresponding to the graph plotted between  $1/k_p$  and  $1/G^n$  are listed in **Table 5.3**. Since the intercepts for  $n \leq 3$  were negative, hence these values were not considered for further analysis. For  $n > 3$ , the slopes and intercept are increasing with constant increase in  $n$ . The plot of  $1/k_p$  versus  $1/G^n$  for  $n = 0.3, 0.5, 0.7, 0.9$  are shown in **Fig. 5.4**. The plot of  $1/k_p$  versus  $1/G^n$  for

remaining values of  $n$  (0.4, 0.6, 0.8, 1.0) were given in Appendix data. All plots give linear regression of  $R^2 > 0.97$ , which demonstrate a reasonable straight line fit, but did not predict satisfactory value of  $a_m$  (experimental mass transfer area). Therefore, further analysis performed for the calculation of  $N$  at different values of  $K$  which was reported in previous literature (Banerjee and Ghoshal, 2016; Geed et al., 2018a; R. K. Sonwani et al., 2019; Swain et al., 2021b).

From Eq. (5.12), the value of  $N$  was calculated at various values of  $n$  and  $K$ . Based on Eq. (5.13), straight line graph were plotted between  $1/k_p$  and  $1/G^n$  which gives slope  $(1/Na_m)$  and intercept  $(1/k_s a_m)$ . These data was further used for calculation of  $a_m$  and  $k_s$ . The obtained values of  $a_m$  and  $k_s$  are listed in **Table 5.4**. The value of  $a_m$  at  $n = 0.7$  and  $K = 5.71$  was calculated theoretically (4.87, Table 5.4) and experimentally (4.6). The close values between theoretical and experimental values were found which clearly indicated that the Eq. (5.13) was working well on present study. For further verification of estimated value of  $n$ ,  $K$ , and  $k_m$  was calculated by Eq. (5.8) using experimental value of  $a_m$ ,  $k_p$  and  $k_s$  for  $K = 5.71$  and  $n = 0.7$ . Eq. (5.11) shows that the plot between  $\ln k_m$  and  $\ln G$  would give slope 'n' and intercept ' $\ln N$ '. **Fig 5.5** shows the change of  $k_m$  with respect to mass flux ( $G$ ) which gives slope 0.7233 and intercept -4.896, respectively. From the intercept, the value of  $N$  was measured to be 0.074 which was very close to the obtained value at  $K = 5.71$  (**Table. 5.4**). From the above result, the mass transfer correlation for biodegradation of BG dye can be proposed as:

$$J_D = 5.71 N_{Re}^{-0.3} \quad (5.21)$$

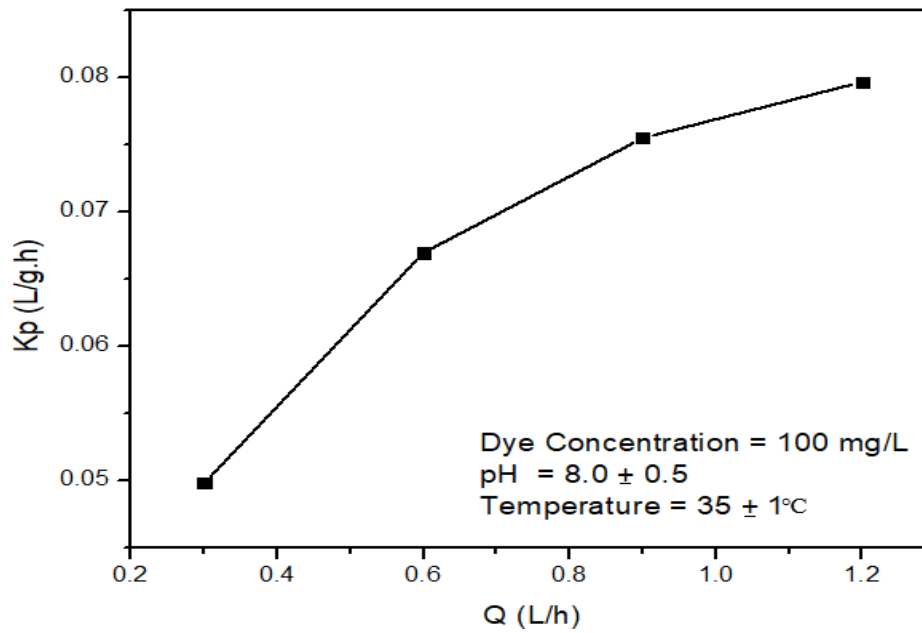


**Fig. 5.3** Effect of different flowrate on the biodegradation rate constant  $k_p$

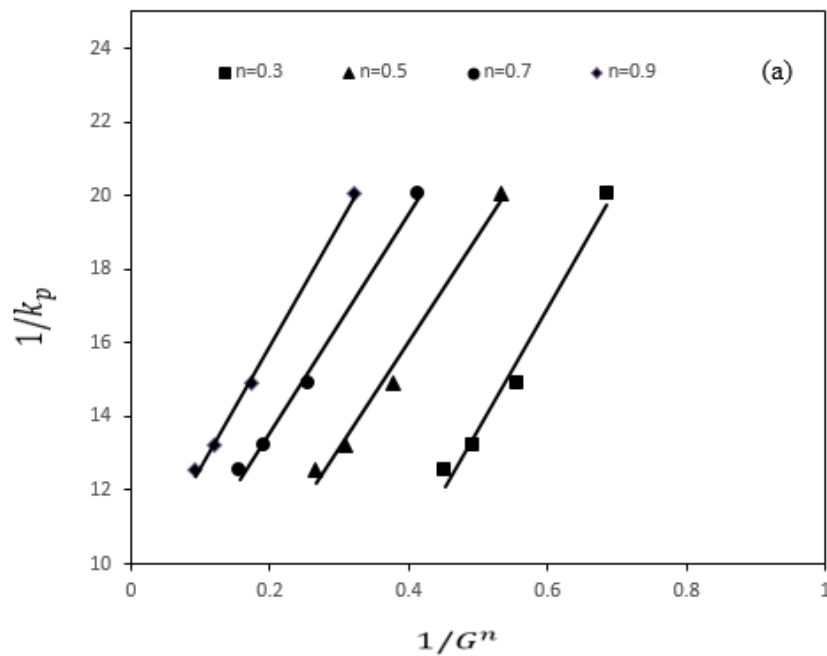


**Fig. 5.4** The plot between  $1/k_p$  and  $1/G^n$  for  $n = 0.3, 0.5, 0.7, 0.9$

**Table 5.2** Experimentally obtained values of  $k_p$ ,  $1/k_p$  and estimated value of  $G$  and  $1/G^n$  at different flowrates.

Q (L/h)	$k_p$ (L/g.h)	$1/k_p$ (g.h/L)	$G$ (g/cm <sup>2</sup> h)	$1/G^{0.1}$	$1/G^{0.2}$	$1/G^{0.3}$	$1/G^{0.4}$	$1/G^{0.5}$	$1/G^{0.6}$	$1/G^{0.7}$	$1/G^{0.8}$	$1/G^{0.9}$	$1/G^1$
0.3	0.049	20.064	3.520	0.881	0.777	0.685	0.604	0.532	0.469	0.414	0.365	0.322	0.284
0.6	0.066	14.930	7.041	0.822	0.676	0.556	0.458	0.376	0.310	0.255	0.209	0.172	0.142
0.9	0.075	13.241	10.562	0.789	0.624	0.493	0.389	0.307	0.243	0.192	0.151	0.119	0.094
1.2	0.079	12.550	14.083	0.767	0.589	0.452	0.347	0.266	0.204	0.157	0.120	0.092	0.071

**Table 5.3** Slope and intercept obtained from a plot of  $1/k_p$  and  $1/G^n$ 

n	0.1	0.2	0.3	0.4	0.5	0.6	0.7	0.8	0.9	1
slope	-	-	-	28.79	29.57	29.178	30.07	31.579	33.622	36.177
intercept	Negative	Negative	Negative	1.757	4.506	6.331	7.628	8.595	9.341	9.99

**Table 5.4** Estimated value of  $N$ , mass transfer area ( $a_m$ ), and intrinsic first-order rate constant ( $k_s$ ) at different values of  $K$  and  $n$ .

n	$K = 1.09$			$K = 1.43$			$K = 1.625$			$K = 2.718$			$K = 5.71$		
	$N \times 10^{-3}$	$a_m$	$k_s \times 10^{-3}$	$N \times 10^{-3}$	$a_m$	$k_s \times 10^{-3}$	$N \times 10^{-3}$	$a_m$	$k_s \times 10^{-3}$	$N \times 10^{-3}$	$a_m$	$k_s \times 10^{-3}$	$N \times 10^{-3}$	$a_m$	$k_s \times 10^{-3}$
0.4	0.3	112.78	5.0	0.3	91.74	6.2	0.4	75.65	7.5	0.7	45.23	12.5	1.6	21.53	26.4
0.5	0.4	67.92	3.2	0.6	55.25	4.0	0.7	45.56	4.8	1.2	27.24	8.1	2.6	12.96	17.1
0.6	0.8	42.58	3.7	0.9	34.63	4.5	1.2	28.56	5.5	2.0	17.07	9.2	4.2	8.12	19.4
0.7	1.3	25.55	5.1	1.6	20.78	6.3	1.9	17.14	7.6	3.2	10.24	12.7	6.8	4.87	26.8
0.8	2.1	15.05	7.7	2.5	12.24	9.5	3.1	10.09	11.5	5.2	6.036	19.2	11.0	2.87	40.4
0.9	3.4	8.74	12.2	4.1	7.11	15.0	5.0	5.86	18.2	8.4	3.507	30.5	17.8	1.66	64.1
1	5.4	5.02	19.9	6.7	4.08	24.4	8.1	3.37	29.6	13.7	2.016	49.6	28.8	0.95	104.2

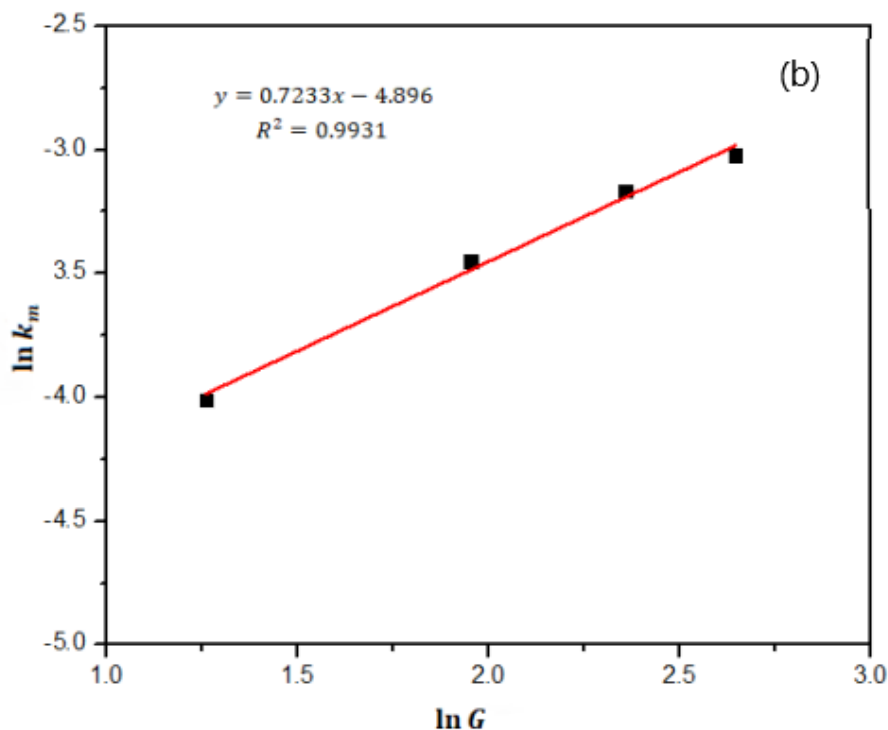


**Fig. 5.5** The plot of  $\ln k_m$  v/s  $\ln G$  for estimation of  $n$  and  $N$

### 5.3.4 FTIR analysis of BG dye before and after biodegradation

FTIR spectrum of control and biologically treated BG dye sample in the wavenumber between  $500 - 4000 \text{ cm}^{-1}$  is analyzed (**Fig 5.6**). Hydroxyl group (O-H) and carboxyl group (C=O) stretch were observed corresponding to wavenumbers of  $3439 \text{ cm}^{-1}$  and  $1737 \text{ cm}^{-1}$ , respectively. The characteristic peak at  $1626 \text{ cm}^{-1}$  attributed to N-H  $1^0$  amine bend, peak at  $1382 \text{ cm}^{-1}$  represent C-H stretch of alkane. Carboxylic acid was corresponding to  $1244 \text{ cm}^{-1}$  and  $1043 \text{ cm}^{-1}$  represent C-N stretch (aliphatic amine). There was a disappearance of peak at

1633  $\text{cm}^{-1}$  and 1147  $\text{cm}^{-1}$  and major shifts in between 1000–1800  $\text{cm}^{-1}$  range of wavenumber which supports successful biodegradation of BG dye (Coşkun et al., 2019).

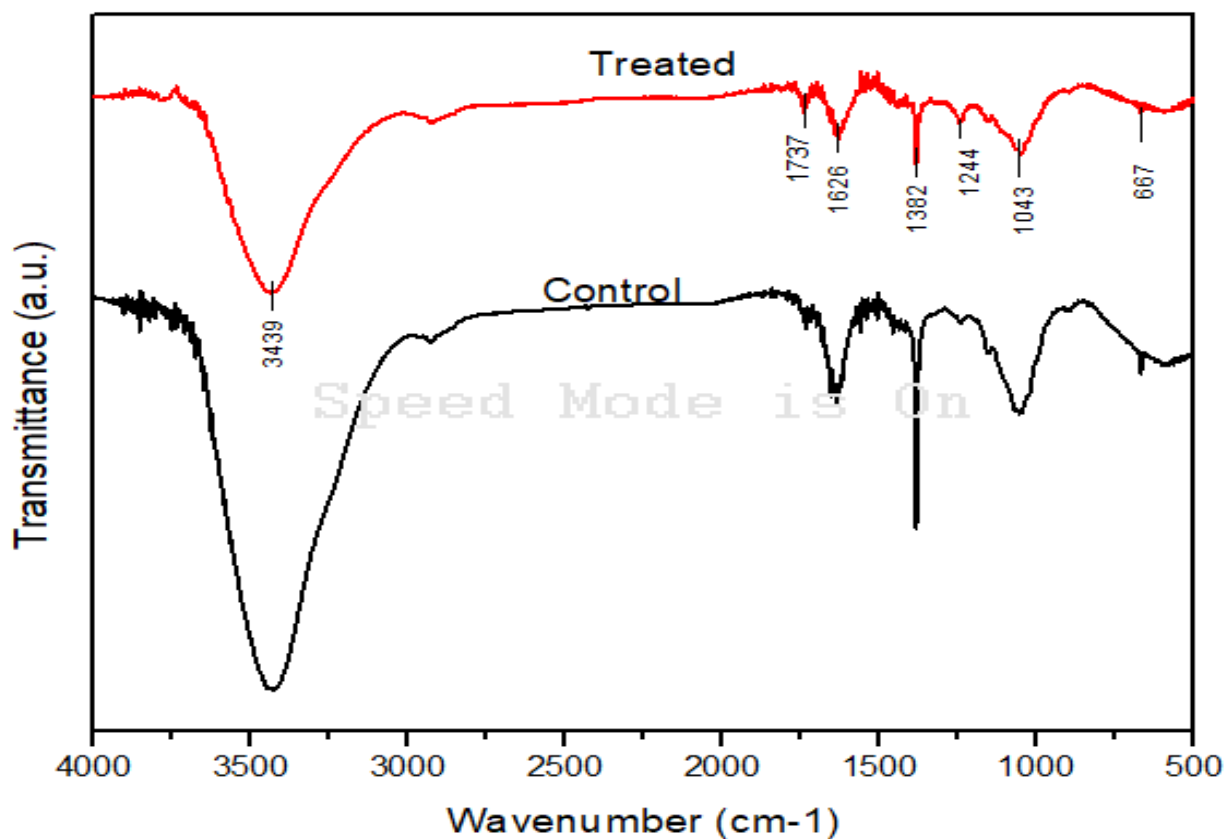
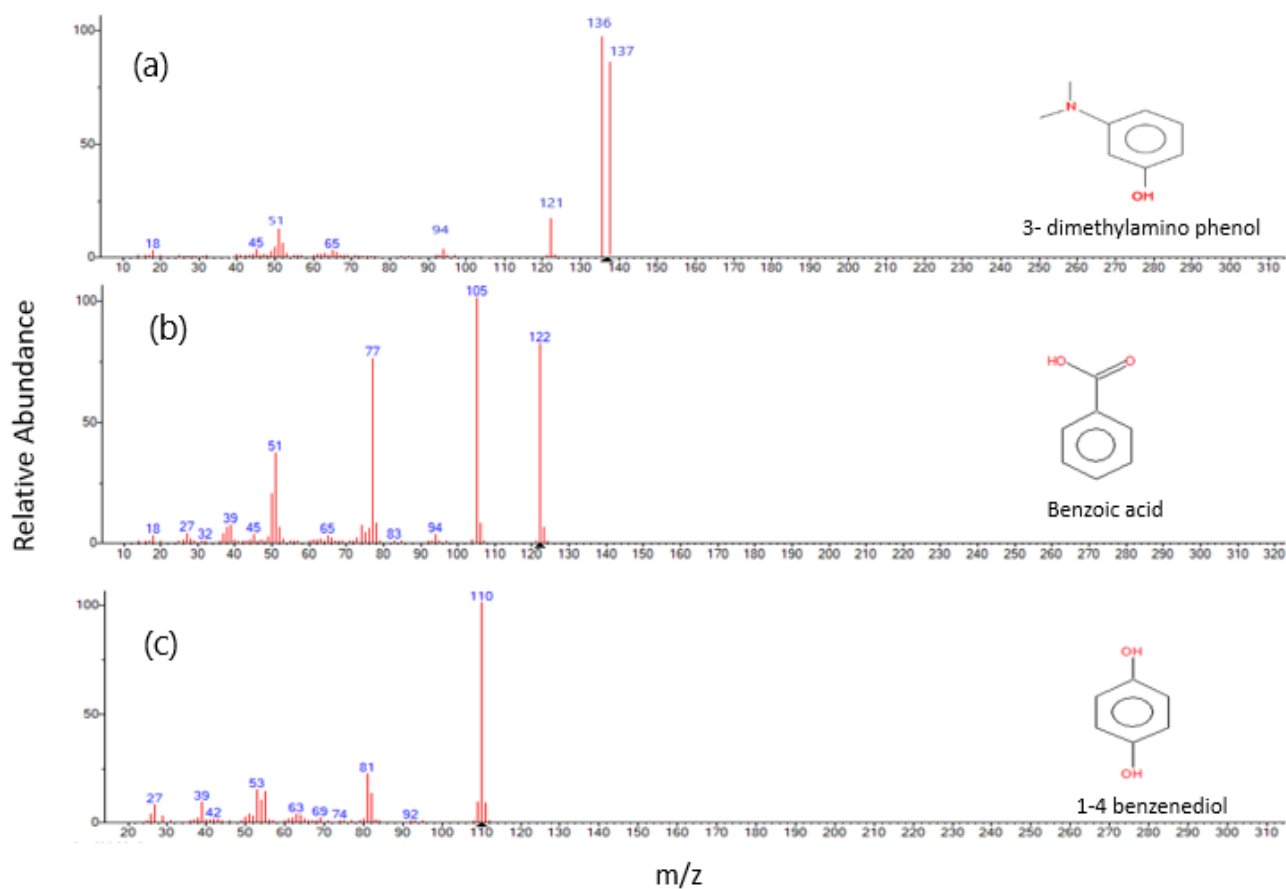


Fig. 5.6 FTIR spectrum of control and treated BG dye sample.

### 5.3.5 Analysis of metabolites and elucidation of degradation pathway

GC-MS analysis was carried to characterize probable metabolites produced during biodegradation of brilliant green dye by *Bacillus licheniformis*. Main metabolites obtained were 3- dimethylamino phenol ( $m/z = 136$ ), benzoic acid ( $m/z = 105$ ), 1-4 benzenediol ( $m/z = 110$ ), and acetaldehyde ( $m/z = 29$ ) as shown in **Fig 5.7**. Other organic compounds were also observed but they were either not part of the degradation pathway or their quantity was very

low and also they were incomparable to previous literature. Based on these metabolites, a metabolic pathway was elucidated for BG dye biodegradation (**Fig 5.8**). In previous literature, it was mentioned that BG first transform into leucobrilliant green by hydrogenation of central carbon atom (Cha et al., 2001; Chaturvedi and Verma, 2015; Song et al., 2020). After that leucobrilliant green degraded into two metabolites: [4-(dimethylamino)phenyl]phenyl and 3-dimethylamino phenol via dibenzocyclization mechanism. Further, 3- dimethylamino phenol probably degraded into 1-4 benzenediol by action of BG reductase and deamination mechanism. These metabolites are generally degraded until the formation of water and CO<sub>2</sub> as the end products.



**Fig. 5.7** Mass spectral profile of metabolites formed after BG dye degradation (a) 3-dimethylamino phenol (b) Benzoic acid (c) 1-4 benzenediol

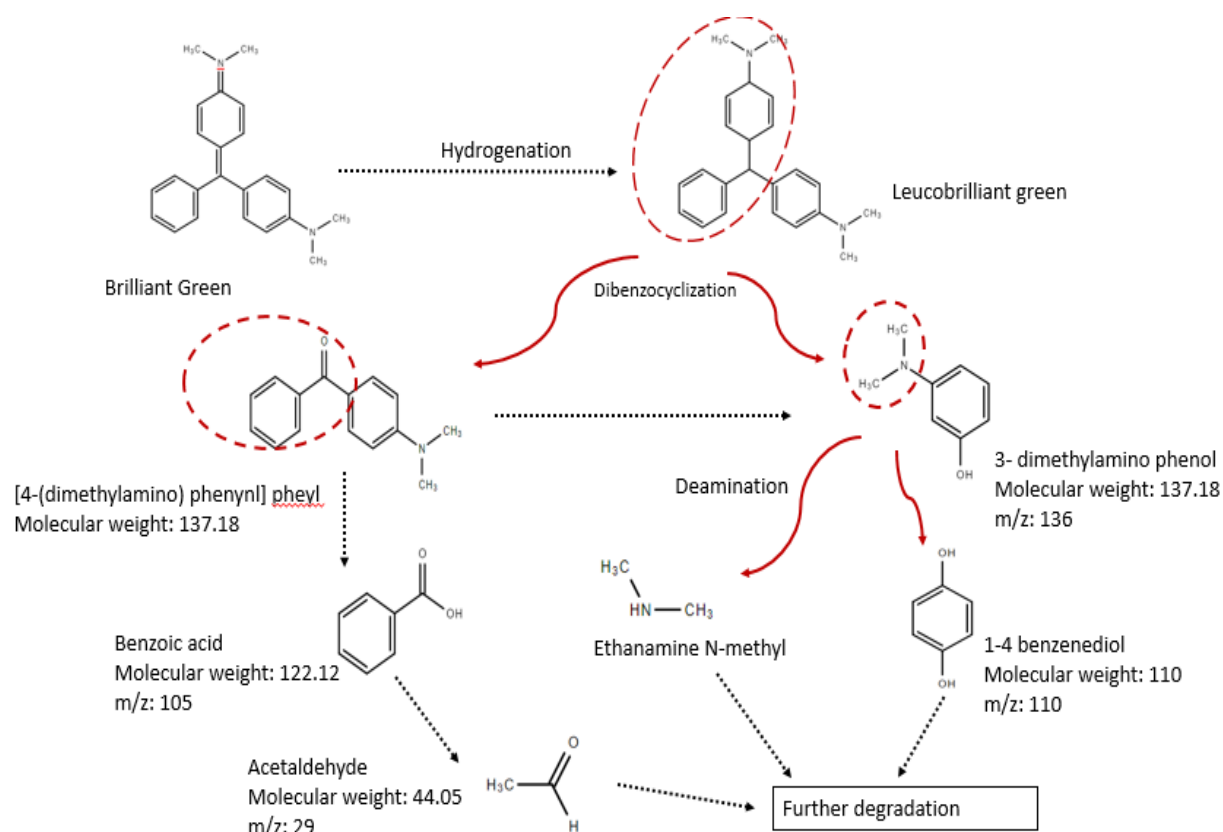


**Fig. 5.8** Proposed pathway for degradation of BG dye by *Bacillus licheniformis* ST5.

### 5.3.6 Kinetic study

The experimentally obtained data of specific growth rate ( $\mu$ ) at various BG dye concentration plotted for the Andrews-Haldane model and Han – Levenspiel models (**Fig 5.9**). Han – Levenspiel model showed better fit with the experimental data. The kinetic parameter obtained from these two models are listed in **Table 5.5**. The kinetics parameter ( $\mu_{max}$  and  $K_S$ ) obtained from Andrew – Haldane model were slightly different from Han – Levenspiel model. The disparity in predicted values between models could be attributed to the fact that the two

---

---

models were initially developed for systems with different microorganisms and substrates (Saravanan et al., 2008). The value of  $\mu_{max}$  and  $K_s$  were estimated as 0.185 (per day) and 115 mg/L, respectively for Han – Levenspiel model. The critical inhibitor concentration ( $S_m$ ) beyond which microorganism ceased to grow was 400 mg/L. The experimental constants ‘ $n$ ’ and ‘ $m$ ’ were found to be 0.7703 and 1.7, respectively. These inhibitory constant values indicated a high efficiency of the bacterial cultures to grow in the presence of BG dye, and thus a complete degradation of the compound. The higher regression coefficient ( $R^2 > 0.98$ ) value showed the suitability of Han – Levenspiel model. The final form of the equation is represented as:

$$\mu = \frac{0.185S \left[1 - \left(\frac{S}{400}\right)\right]^{0.7703}}{S + 115 \left[1 - \left(\frac{S}{400}\right)\right]^{1.7}} \quad (5.22)$$

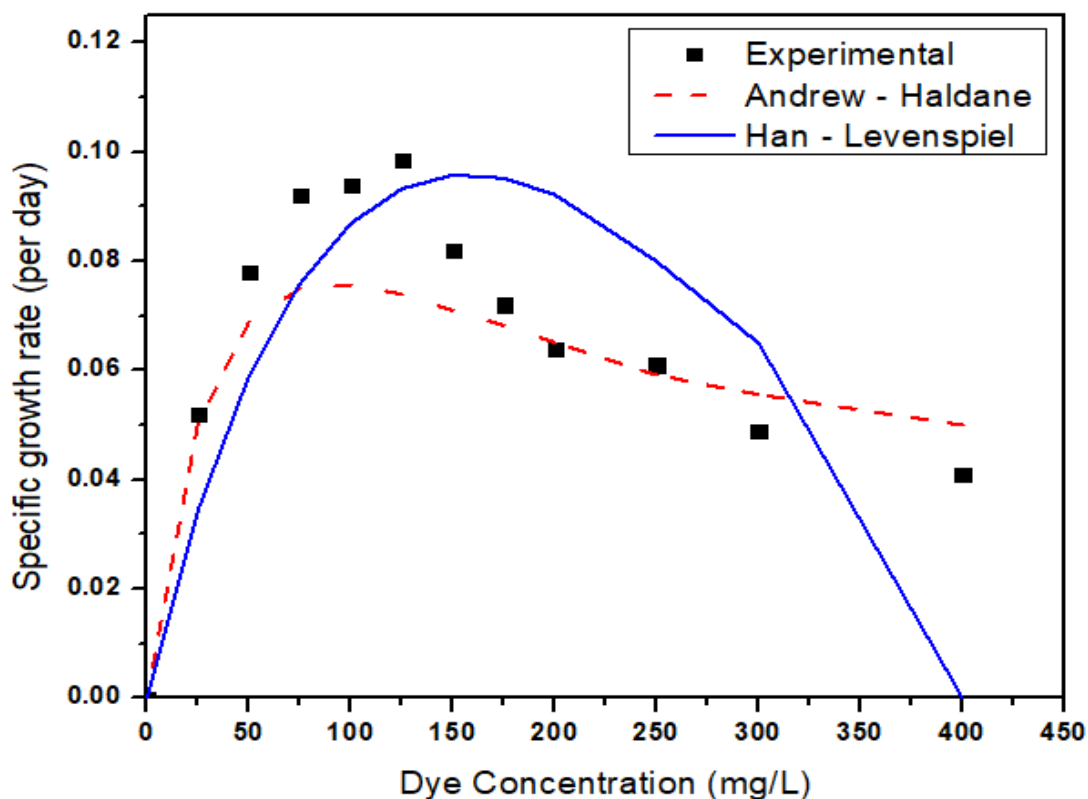


**Fig. 5.9** Experimental and predicted plot for specific growth rate by Andrew – Haldane and Han – Levenspiel model.

**Table 5.5** Values of kinetics parameter obtained using Andrew – Haldane and Han – Levenspiel model.

Dye Concentration (mg/L)	Model	$\mu_{\max}$ (per day)	$K_s$ (mg/L)	$K_i$ (mg/L)	$S_m$	$n$	$m$	$R^2$
0-400	Andrews-Haldane	0.158	50.0	170	-	-	-	0.84
0-400	Han – Levenspiel	0.185	115	-	400	0.7703	1.7	0.98

$\mu_{\max}$ : Max specific growth (per day);  $K_s$ : Half-saturation constant (mg/L);  $K_i$ : inhibition constant (mg/L);

$S_m$ : Critical inhibitor concentration.

### 5.3.7 Toxicity Studies

#### 5.3.7.1 Phytotoxicity analysis

To assess the toxicity level of our biologically treated dye sample, phytotoxicity test was performed using *vigna radiata* seeds. Outcome of the analysis was compared by %germination, root and shoot lengths for biologically treated (BT) and untreated (UT) dye wastewater. *Vigna radiata* seeds irrigated with UT BG dye solution (100 mg/L) showed low germination (31.4%) as compared to seeds which were irrigated with BT (germination = 86.1%) as shown in **Fig. 5.10**. Further shoot (plumule) and root (radicle) lengths were also found relatively lower for UT wastewater (1.12 cm and 0.87 cm, respectively) than BT wastewater (9.33 cm and 4.31 cm, respectively). The obtained results clearly indicate that BG dye phytotoxicity was significantly removed by biological treatment.

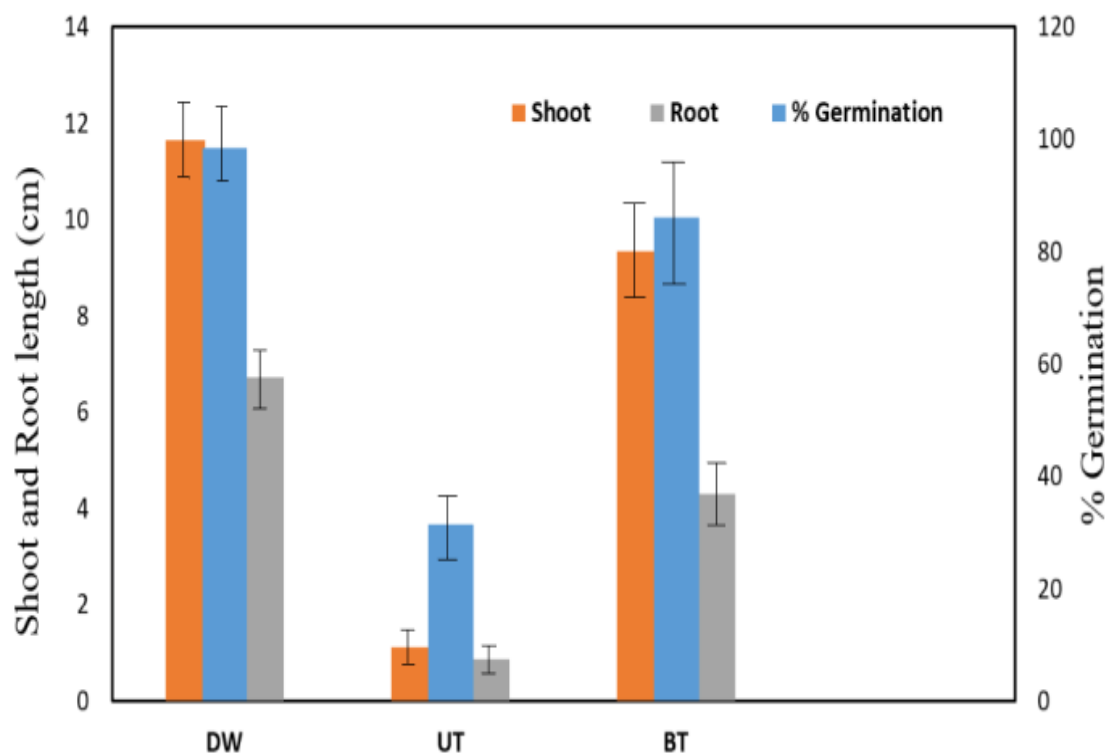


**Fig. 5.10** Comparison of % Germination, shoot, and root length for DW, UT, and BT samples.

### 5.3.7.2 Bacterial analysis

The bacterial toxicity test was performed by measuring bioluminescent intensity of *P. luminescent* bacteria in different samples (i.e. DW, UT and BT). After bioluminescent bacteria were inoculated, acute and chronic toxicity were evaluated after 15 min and 16 h, respectively. 1000  $\mu\text{L}$  of *Photobacterium luminescence subsp. Akhurstii* was added to 5 mL of different sample comprised of DW, UT and BT for bioluminescence measurement. It is clearly visible that after acute exposure, the bioluminescence intensity of *P. luminescence* at 512 nm was decreased for UT sample ( $1.8 \times 10^6$  cps) in comparison to DW sample ( $3.6 \times 10^6$  cps) (**Fig 5.11**

(a)). Bioluminescence intensity of BT sample was increased from  $1.8 \times 10^6 - 3.1 \times 10^6$  cps, which was close to the DW sample value. This indicates that acute toxicity of BT sample reduced significantly and become comparable to DW sample.

The chronic exposure of BT sample ( $1.5 \times 10^6$ ) showed improvement in bioluminescence intensity in comparison to UT sample ( $0.5 \times 10^6$ ) (**Fig 5.11 (b)**). This can be attributed to enhanced degradation of toxic byproduct (such as amine) by biological treatment and also improved degree of mineralization. The bioluminescence inhibition of BT and UT sample were calculated at 512 nm. After acute exposure, BT sample showed only 12.7% bioluminescence inhibition while UT sample showed 48.4% inhibition. For chronic exposure, bioluminescence inhibition was 37.6% for BT sample and 77.9% for UT sample, which indicate towards enhanced bacterial mortality of BT sample in comparison to UT sample for acute and chronic exposure.

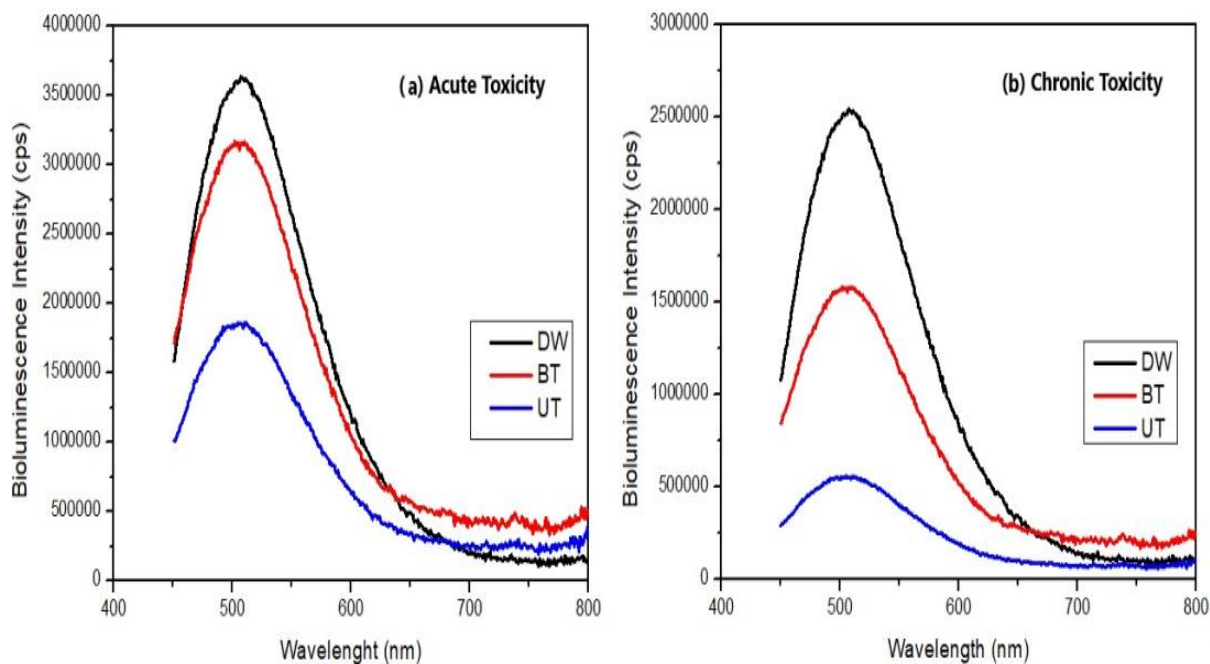


**Fig.5.11** . (a) Acute bioluminescence intensity for DW, BT and UT samples (b) Chronic bioluminescence intensity for DW, BT and UT samples.

#### 5.4 Conclusions

The effect of external film diffusion on biodegradation rate was investigated at various flow rates (0.3 – 1.2 L/h). The biodegradation rate of BG dye was found to be dependent on influent flow rate. The identification of metabolites such as 3-dimethylamino phenol, Benzoic acid, 1-4 benzenediol and acetaldehyde confirms successful biodegradation of BG dye. A metabolic pathway was proposed for bacterial degradation of BG dye. A new correlation  $J_D = 5.71 N_{Re}^{-0.3}$  was proposed which successfully predicts the experimental data for the biodegradation of BG dye. This correlation can be beneficial for scale-up and designing of

PBBR for dye degradation. Biologically treated samples show less toxicity towards *vigna radiata* seeds and *P. luminescence* bacteria in comparison to untreated sample. Treated water can be further used for various purposes such as: irrigation, domestic use, sanitation etc.